Journal of Visualization, Vol.6, No.1 (2003) 67−76

Flying Characteristics and Flow Pattern of a Sphere with Dimples

Aoki, K. *1, Ohike, A.*2, Yamaguchi, K. *3 and Nakayama, Y. *4

*1 Tokai University, Department of Mechanical Engineering, School of Engineering,1117 Kitakaname, Hiratsuka, Kanagawa, 259-1292, Japan.
*2 Nissan Motor Co., Ltd., 560-2 Okatsukoku, Atsugi, Kanagawa, 243-0192, Japan.
*3 The Yokohama Rubber Co., Ltd., 2-1 Oiwake, Hiratsuka, Kanagawa, 254-8601, Japan.
*4 Future Technology Research Institute, 3-56-2 Higashi-Oizumi, Nerima, Tokyo, 178-0063, Japan.

Received 23 May 2002
Revised 30 August 2002

Abstract : It is known that the flying characteristics of the golf ball is influenced by flying speed, rotational frequencies and the dimples, etc. In this study, the drag and lift acting on the test balls are measured using a three components loadcell by changing Reynolds number and the spin rate ratio, the number and the depth of dimples. And the flow around the balls is visualized by applying the oil film method and PIV in the stationary state. From these results, the aerodynamic drag and lift coefficients of the balls in the stationary and the rotational state are made clear.

Keywords : Golf ball, Dimple, Drag and lift characteristics, Visualization

1. Introduction

The flying distance and the trajectory of a golf ball is known to be affected by initial velocity and the spin given at the time of impact, the aerodynamic resistance and the environmental conditions during the flying time. As far as the flight of the golf ball is concerned, Bearman and Harvey(1976), Smits and Smith(1994) have written studies of the drag and lift characteristics, the spin rate decay, and so on. But, there has been no study on the influence that the dimple structure on a spherical surface has on its flying characteristics.

The aim of this study is to clarify the relation between the flying characteristics and the number and the depth of dimples, in the case of the stationary and the rotating state. The number of dimples is changed from 0 (smooth) to 504 using test balls. The drag and lift acting on a stationary and a rotating test ball are measured by changing Reynolds number from 3.0×10^4 to 1.3×10^5 and the spin rate ratio from 0.05 to 0.6 in a uniform airflow. And, these data are compared and examined. Visualizing the flow around the test balls in the stationary state, the separation point and the flow pattern are made clear.

2. Experimental Apparatus and Method

2.1 Test Balls

The test balls are made of vinyl chloride and their diameter d is 42.6 mm having a similar diameter to real Golf balls. The size and shape of dimples are shown in Fig. 1. In this experiment, the ratio of the depth to width k/c (=0.096 remains constant and the number of dimples N_D is varied from 104 to 504. And, in another case with N_D =328, the depth of dimple k is also varied (k/c =0.183). The main specifications of the spherical surfaces are shown in Table 1.

Table 1. Specifications of spherical surfaces.

N_D	b [mm]	c [mm]	k [mm]
smooth	-	-	-
104	3.897	3.528	0.338
184	2.043		
328	0.650		
504	0.297	3.046	0.292
328deep	0.650	3.528	0.646

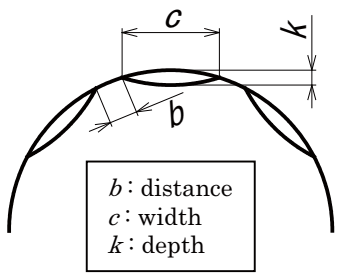

Fig. 1. Sectional-view of dimple.

2.2 Experimental Apparatus and the Data Processing

Experimental apparatus is shown in Fig. 2. A frame covers the central part of the test section in the suction type wind tunnel, providing a uniform airflow. A ball is fixed at the center of the test section using a piano wire, giving a tension on both fixed ends. The drag D and the lift L acting on the ball are measured using the three components loadcell. In the case of the rotating state, the vertical shaft connects to a motor at the lower fixed end. The diameter of the piano wire is 1/16 inch (=1.58 mm) in the case of the stationary state and 1/32 inch (=0.79 mm) in the case of the rotating state, which have a negligible interference effect on the drag measurement. In the experiment, D and L are measured for the spin rate ratio α ($=\pi dN/60U$: the peripheral velocity to the velocity through the airflow), changing the flow velocity U in the wind tunnel ranging from 10 to 45 m/s and the motor's rotating speed N ranging from 1,000 to 4,000 rpm.

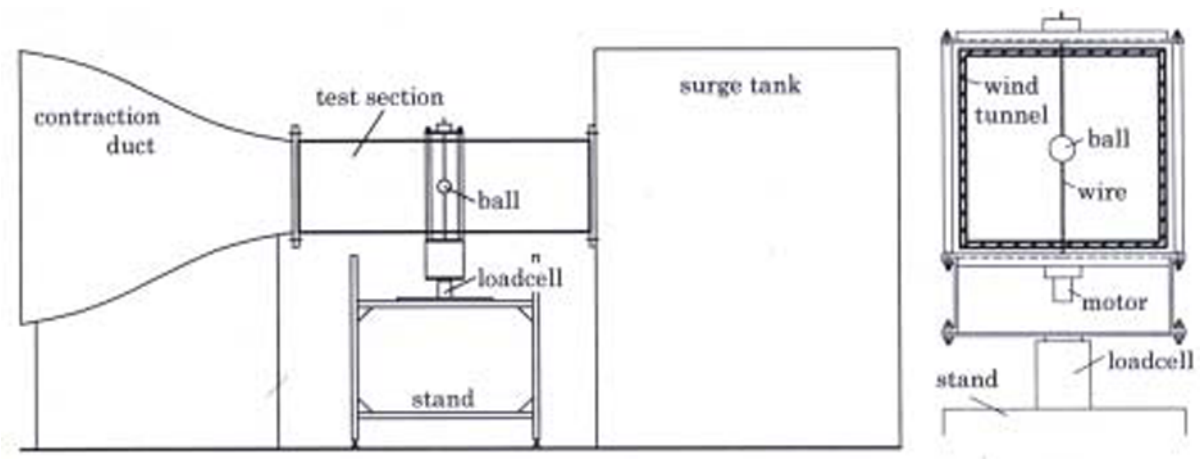

Fig. 2. Measuring equipment. (outline and sectional-view)

The resultant values are calculated by subtracting the values measured using only the piano wire from those obtained in the experiment. D and L are estimated by taking the mean value of 1600 strain data at every 1.25×10^{-3} s interval using the strain gage capable of measuring three components of the force. From these values, the drag and the lift coefficient C_D and C_L are calculated based on the following equations.

$$C_D = \frac{D}{(1/2)A\rho U^2} \tag{1}$$

$$C_L = \frac{L}{(1/2)A\rho U^2} \tag{2}$$

where A[m^2] is spherical projection area, and ρ [kg/m^3] is density.

2.3 PIV (Particle Imaging Velocimetry) and Visualizing Experiment Method

2.3.1 PIV Measurement Technique

First, the tracer particles (the smoke) are supplied from the intake before the test section of the wind tunnel. The laser light sheet made of YAG laser (30mJ, Double YAG, 150Hz) is projected to the test section along the flow and the movement of the tracer particles is captured with CCD camera. Then, the velocity vector and the vorticity are calculated by the correlation method from the particle pictures and the wake of the ball is made clear.

2.3.2 Oil Film Method

The material of the oil film is made by mixing the liquid paraffin with the pigment like titanium dioxide and adding the oleic acid. This oil film is brushed uniformly and thinly on the ball surface.

3. Experimental Results and Discussion

3.1 Characteristics of the Stationary Balls with Dimples

Fig. 3 shows the comparison of C_D for a ball with and without dimples in terms of Reynolds number Re ($=Ud/\nu$; ν : kinematic viscosity). The values of C_D of the smooth ball become stable with 0.4~0.5 and this region belongs to the subcritical region. This result shows a good agreement with the other results not shown here. Generally, the smooth ball reaches a critical region with $Re=3.5\times10^5$ and C_D decreases to less than 0.1. For higher Re, C_D approaches to 0.2 and the region becomes the super-critical region.

For any balls with dimples, on the other hand, it can be confirmed that there also exist the subcritical, critical and super-critical regions in terms of Re. Putting dimples on a spherical surface shifts the critical region toward the lower Re direction in comparison with the smooth ball. Furthermore in the case of $N_D=104\sim328$, as N_D becomes larger, the critical region shifts toward the lower Re direction. In the case when N_D is 328 and over, the changes of C_D in terms of Re show the same trend. The reason for this may be that the boundary layer near separation point on the ball surface is disturbed by the dimples and changes to turbulent flow. Consequently the separation point moves to the downstream(Oki et al., 1998). But, as for the mechanism that the critical region moves by the influence of N_D, more detailed research will be required in order to identify the exact flow condition.

When N_D is kept the same and only k is varied, the critical region also shifts toward the lower

Re direction and C_D increases in the super-critical region as *k* becomes deeper. The reason for this may be that as *k* becomes deeper, the effect of the flow inside a dimple becomes larger. The flow near the separation point may thus change to turbulent flow at the lower *Re* direction and this effect would continue to higher *Re* region.

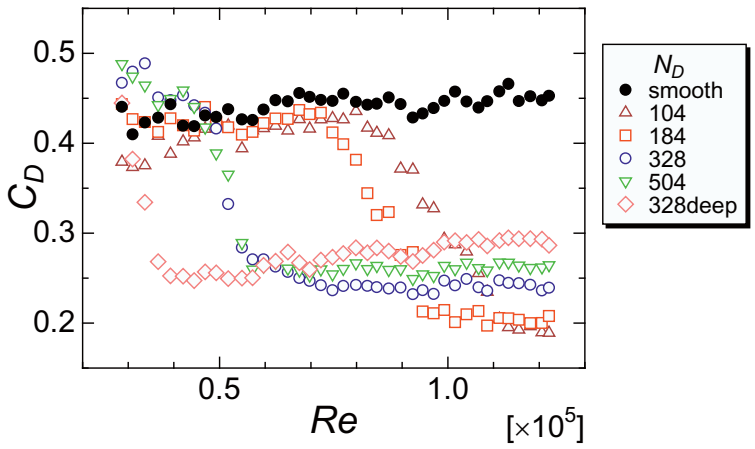

Fig. 3. Change of drag coefficient to Reynolds number.

Figure 4 shows the change of C_D and C_L to *Re* for N_D =184. In the subcritical region under *Re* =6.0×10⁴ and the super-critical region beyond *Re* =9.5×10⁴, the fluctuation of C_L is small and the value of C_L can be regarded as approximately 0. However, the fluctuation of C_L becomes larger in the critical region, especially in the regions of the transition from subcritical to critical and from critical to super-critical. The reason for this increasing fluctuation can be considered as follows. In the entrance of the critical region, the flow becomes irregular at the early stage of turbulence. This phenomenon occurs first at the entrance of the critical region. By chance, the time when the turbulence occurs is slightly different between at the upper side and lower side of the ball. This is the reason why the value of C_L becomes maximum in this region. These transient phenomena continue in the critical region. At the end of the critical region, the turbulence becomes a balanced state at one side and at the other side it continues as an unbalanced state. So, the lift becomes large again in this region. It is this asymmetrical flow in the critical region that produces the lift on the ball.

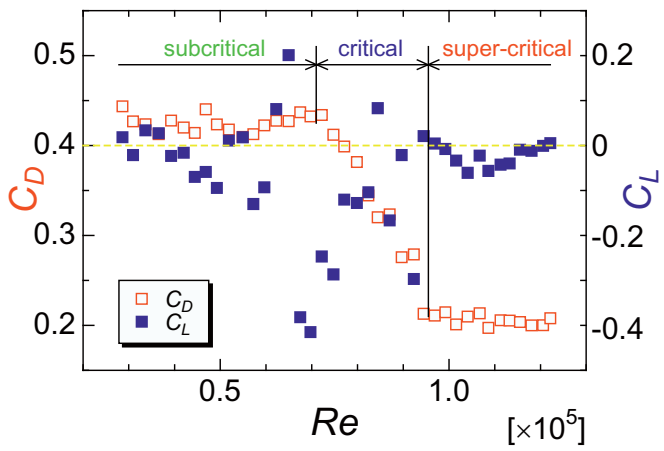

Fig. 4. Change of drag and lift coefficient to Reynolds number. [N_D=184]

3.2 PIV and the Observation by the Visualizing Experiment

Figures 5 (a),(b), and (c) are the figures analyzed by PIV and photographs taken by using the oil film method, corresponding respectively to Re =4.3×10⁴,8.5×10⁴,1.2×10⁵ for N_D =184. Comparing them with Fig. 3, the following results are obtained. From Fig. 5 (a) obtained by the oil film method, the separation angle θ_S (the angle measured from the horizontal plane) is 80° in the subcritical region. θ_S moves to 85~95° in the critical region as shown in Fig. 5 (b) and it becomes about 100° in the super-critical region as shown in Fig. 5 (c).

In the figures, the flow velocity becomes slower as the color turns to blue from red, and the direction of a vector is the flow direction. From the velocity distributions analyzed by using PIV, it becomes clear that as Re increases for the same ball, the separation point of the ball moves downstream and then the wake (the reverse flow region) lessens. Consequently, it is thought that C_D also decreases. And, in the critical region, the asymmetrical pattern of the wake becomes large as explained in *3.1*.

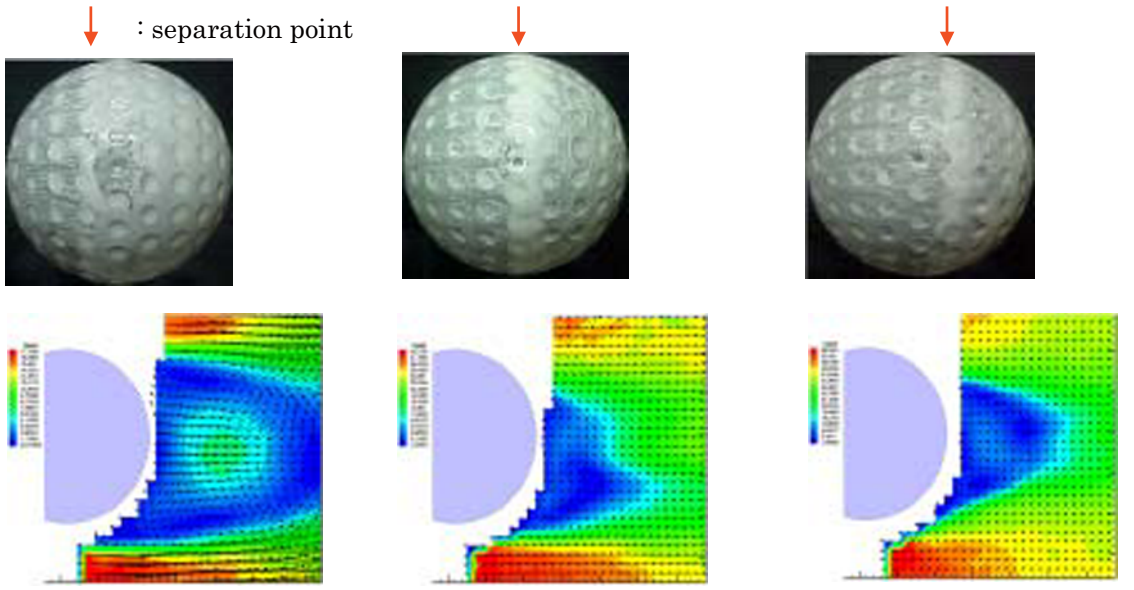

(a) Re =4.3×10⁴, subcritical [θ_S =80°, C_D =0.42]
(b) Re =8.5×10⁴, critical [θ_S =85~95°, C_D =0.32]
(c) Re =1.2×10⁵, super-critical [θ_S =90~100°, C_D =0.20]

Fig. 5. Visualization around Ball by PIV and Oil Film Method. [N_D=184]

Figures 6 (a), (b), and(c) show flow visualization results using the oil film method, corresponding respectively to N_D =0 (smooth), 184, 328 for Re =8.5×10⁴. From these photographs, it is clear that θ_S changes according to N_D, changing the flow region. The change of θ_S to N_D for various Re is shown in Fig. 7. From these results, it is found that θ_S is about 80° in the subcritical region; it ranges from approximately 80° to 100° in the critical region; and it becomes about 100° in the super-critical region.

Figures 8 (a) and (b) are the photographs taken by the oil film method in the critical region for N_D=104. (a) is a photograph taken from the left side and (b) is a photograph taken from the right side watching from the upstream. Comparing(a) with (b), it can be recognized clearly that in this case the separation point on the left hand side surface of the ball moves to rearward further than on the right hand side. From these phenomena, the flow of both sides becomes asymmetric and then the lift appears as explained in *3.1*.

(a) smooth, subcritical [θ_S=79°, C_D=0.44]

(b) ND=184, critical [θ_S=85~95°, C_D=0.32]

(c) ND=328, super-critical [θ_S=97~106°, C_D=0.24]

Fig. 6. Visualization of Separation Point by Oil Film Method. [Re=8.5×10^4]

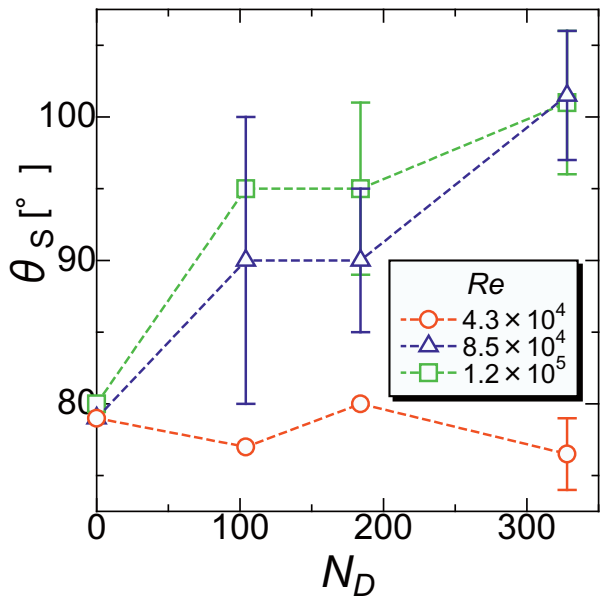

Fig. 7. Separation Point to Number of Dimples.

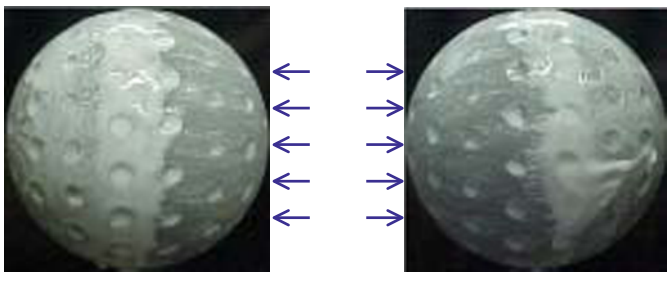

(a) left hand side (b) right hand side

Fig. 8. Visualization of Side-view of Ball by Oil Film Method. [N_D=104, Re=8.5×10^4]

3.3 Characteristics of the Rotating Balls with Dimples

Figure 9 shows the change of C_D and C_L to α for N_D =184, with Re as the parameter. Re =4.3×10^4, 8.5×10^4 and 1.3×10^5 respectively belong to the subcritical, critical and super-critical region in the stationary state. Based on this finding, it is considered that the difference of trend in Fig. 9 is not due to the flow velocities, but due to the regions in the stationary state. Therefore, after this, the aerodynamic drag and lift characteristics are examined for every region.

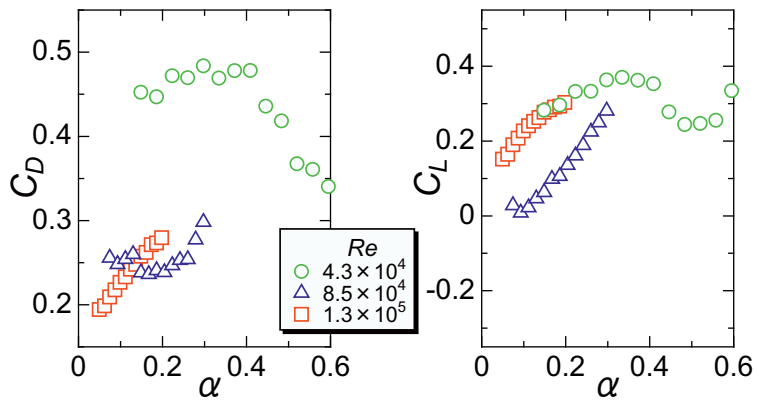

Fig. 9. Change of drag and lift coefficient to spin rate ratio. [Effect of Reynolds number, N_D=184]

Figure 10 shows the change of C_D and C_L to α, having N_D and Re as parameter. The following results are obtained. In the subcritical region as shown in Fig. 10 (a), as α increases, both C_D and C_L tend to decrease after increasing a little for all parameters. As far as the smooth ball is concerned, it can be confirmed that the negative lift (the negative Magnus force) appears at α=0.3. This result agrees with the experimental result by Taneda(1957). The reason for this may be as follows. The flow on the acceleration side becomes the laminar flow, and the separation point moves to the upstream side. However, the flow on the deceleration side becomes the turbulent flow, and the separation point moves to the downstream side. These phenomena are known as the phenomena to appear in the critical region of the stationary state. In the super-critical region as shown in Fig. 10 (c), as α increases, both C_D and C_L tend to increase uniformly. And they are almost the same value in terms of α. Moreover, when N_D is 328 and 504, both plots overlap. The reason may simply be that the value of C_D in terms of Re agrees in the stationary state. In the critical region, as shown in Fig. 10 (b), both C_D and C_L don't show a clear trend as in other regions. Their value is scattered for all balls. However, roughly speaking, it can be surmised that they tend to increase after decreasing as α increases. The reason for this may be that the critical region is very unstable, where the value of C_D suddenly decreases and the fluctuation of C_L is large.

Figure 11 shows the change of C_D and C_L in terms of α in the super-critical region, when N_D is 328 and k is varied, with Re as the parameter. From this figure, as k becomes shallower, the values of C_D in terms of α become smaller as in the stationary state: the aerodynamic resistance lessens. And the values of C_L become larger contrary to the case of C_D. The lift is thus produced more easily. In addition, when Re is varied, the change of both C_D and C_L is similar in value in the ball with shallower dimples. However, as Re becomes larger, the values of C_L decreases significantly with deeper dimples: the lift is produced with more difficultly.

The present results generally show a good agreement with the trend of Smits and Smith(1994) results. As for differences of the values in flow ranges, it is considered that they are affected very significantly by differences of N_D. But, to understand the mechanism by which the number of dimples influences the flying characteristics, more detailed research will be required.

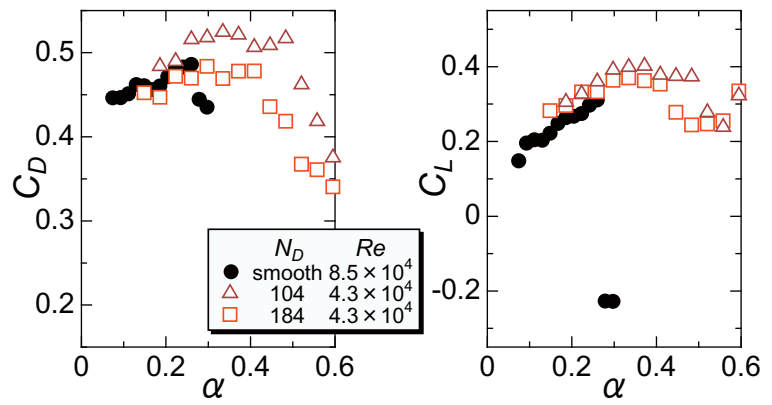

(a) subcritical

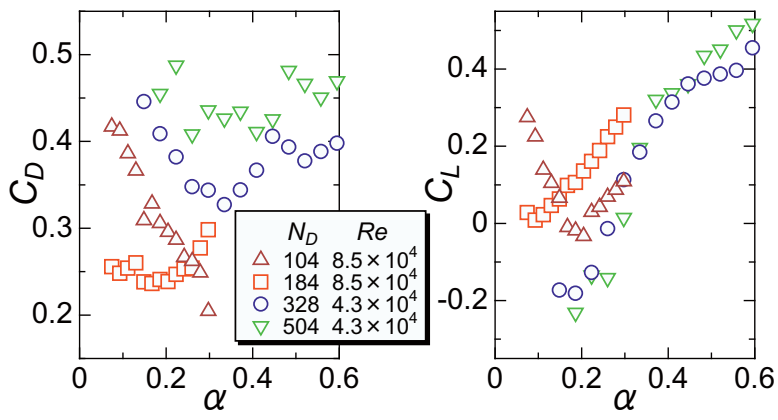

(b) critical

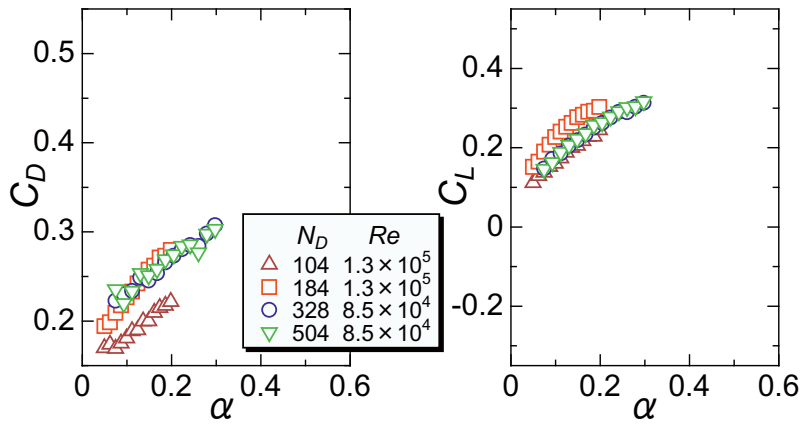

(c) super-critical

Fig. 10. Change of drag and lift coefficient to spin rate ratio. [Effect of region]

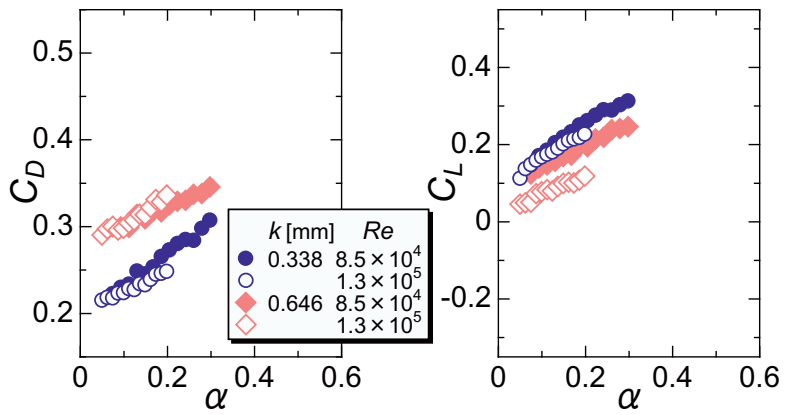

Fig. 11. Change of drag and lift coefficient to spin rate ratio. [Effect of depth, N_D=328]

4. Conclusion

From the analysis of the experimental results, the following results are obtained.

(1) Putting dimples on a spherical surface shifts the critical region toward the lower *Re* direction in comparison with the smooth ball. Moreover, as N_D becomes larger in the case of N_D=104~328 and *k* becomes deeper, the critical region shifts toward the lower *Re* direction.

(2) In the case when N_D is 328 and over, the changes of C_D in terms of *Re* show the same trend.

(3) In the critical region, the fluctuation of C_L becomes larger, especially at the transition of the regions from subcritical to critical.

(4) As *Re* increases in the case of the same ball, the separation point of balls moves downstream, and then the wake area becomes smaller. Consequently C_D also becomes smaller.

(5) The separation angle θ_S is about 80º in the subcritical region. It ranges from approximately 80º to 100º in the critical region, and it becomes about 100º in the super-critical region.

(6) The aerodynamic characteristic of a rotating ball with dimples is affected by the characteristics (regions) in the stationary state.

(7) In the subcritical region, as α increases, both C_D and C_L tend to decrease after having increased a little for all parameters. And in the super-critical region, as α increase, both C_D and C_L tend to increase uniformly.

(8) As the depth of dimples is shallower, in the super-critical and rotational state, the aerodynamic resistance becomes smaller and the lift is produced more easily.

Acknowledgments

The authors would like to thank Ms. Yasue Tanaka of KANOMAX JAPAN. INC. for her support in conducting the present study of PIV using a new PIV system of the same company.

References

Bearman, P. W. and Harvey, J. K., Golf Ball Aerodynamics, Aeronautical Quarterly 27, (1976), 112-122.
Oki, M., Aoki, K. and Nakayama, Y., Flow Characteristics and around a Circular Cylinder with Groove, JSME, 64-625, (1998), 2868-2873.
Smits, A. J. and Smith, D. R., A New Aerodynamics Model of Golf Ball in Flight, Science and Golf II, (1994), 340-347.
Taneda, S., Negative Magnus Effect, Reports of Research Institute for Applied Mechanics, Vol. V, No. 20, (1957), 123-128.

Author Profile

Katsumi Aoki: He received his M.Sc. (Eng.) degree in Mechanical Engineering in 1967 from Tokai University and his Ph.D. in Mechanical Engineering in 1986 from the same University. After obtaining M.Sc. he worked as a research assistant, a lecturer, and an associate professor at Tokai University before taking up his current position as a professor of Tokai University. His current research interest covers flow around a rotating circular cylinder with and without grooves, flow around a rotating sphere, possibility of drag reduction using triangle-type cavity and flow visualization by spark tracing method of complicated flow field like in centrifugal blower.

Atsuo Ohike: He received his B.Sc. (Eng.) degree in Mechanical Engineering in 2000 and his M.Sc. (Eng.) in 2002 from Tokai University. He is currently employed in Nissan Motor Co., Ltd.

Kiyonaga Yamaguchi: He received his B.Sc.(Eng.) degree in Polymer Chemistry in 1975 and his M.Sc.(Eng.) in 1977 both from Kyoto University. He is currently employed in The Yokohama Rubber Co.,Ltd.

Yasuki Nakayama: He received his B.Sc. (Eng.) degree in Mechanical Engineering in 1952 from Waseda University, and his Ph.D. in Mechanical Engineering from same University in 1963. He joined the National Railway Research Institute and conducted many research investigations in the area of fluid mechanics. He then became a Professor of Tokai University, where he taught and researched fluid mechanics and visualization. He holds President of the Future Technology Research Institute concurrently. He has received many distinctions and awards for his outstanding research. He has been a visiting Professor of Southampton University, UK, President of The Visualization Society of Japan, and Director of The Japan Society of Mechanical Engineers. He has published 10 books and more than 160 research papers.